光学学报

2 μm Tm:$GdScO_3$锁模激光器

魏文龙[1]，张宁[1]，宋青松[2]，刘坚[1]，王占新[1]，赵永光[1*]，徐晓东[1]，薛艳艳[2]，徐军[2]

[1]江苏师范大学江苏省先进激光材料与器件重点实验室，江苏 徐州 221116；

[2]同济大学高等研究院物理科学与工程学院，上海 200092

摘要 钙钛矿结构的新型 Tm:$GdScO_3$晶体具有平坦且宽带(>450 nm)的增益光谱，可以产生 2 μm 波段少周期激光脉冲。然而，目前该晶体的锁模激光特性，尤其是其各向异性的超短脉冲输出特性尚未明朗。采用b切的 Tm:$GdScO_3$晶体作为增益介质，通过共振泵浦被动锁模技术，详细研究了其$E//a$发光方向的飞秒脉冲输出特性，实现了 60 fs 激光脉冲产生(约 9 个光学周期)，激光中心波长为 2034 nm，光谱半峰全宽为 80 nm，时间带宽积为 0.35，接近傅里叶转换极限。该研究证明了 Tm:$GdScO_3$晶体是实现 2 μm 波段少周期飞秒脉冲的理想激光材料，所获得的飞秒激光在分子超快动力学、高分辨率分子光谱学等科学研究领域极具应用潜力。

关键词 固体锁模激光器；Tm:$GdScO_3$晶体；超短脉冲

中图分类号 O436 **文献标志码** A **DOI**: 10.3788/AOS231115

1 引 言

2 μm 波段的飞秒激光脉冲在分子超快动力学研究[1]、高精度有机材料加工[2]、自由空间光通信[3]等领域具有重要的应用潜力，也可作为光参量振荡器的泵浦源通过频率下转换来产生中远红外激光[4]，是当前激光技术领域的前沿热点。20 世纪 80 年代，随着半导体制备工艺的商业化以及新型低维材料的快速发展，具有高信噪比、载波包络稳定、高效率等优势的被动锁模固体激光器逐步成为获得飞秒脉冲的主要手段之一。其中，基于稀土铥(Tm)和钬(Ho)离子的激光材料是产生 2 μm 激光的主要增益介质[5-7]。然而，自从 1991 年美国海军实验室第一次实现 2 μm 固体激光锁模(35 ps)[8]，往后的 20 多年，该波段固体锁模激光脉冲始终无法突破 100 fs。直到 2017 年，德国马克斯·玻恩研究所 Petrov 课题组首次在固体锁模激光器中产生了低于 100 fs 的脉冲，所采用的泵浦源为波长 796 nm 的钛宝石激光器，增益介质为单斜的 Tm:$MgWO_4$晶体，以石墨烯作为可饱和吸收体最终实现 86 fs 脉冲产生，激光中心波长为 2017 nm，光谱半峰全宽(FWHM)为 53 nm[9]。目前，国内外科研工作者开展了一系列 2 μm 超快激光材料和激光技术方面的探索工作，并取得重要进展。

目前，在基于 Tm/Ho 单掺或共掺的激光材料中，能够实现 100 fs 脉冲输出的基质材料主要有：倍半氧化物(Re_2O_3，Re 为 Lu、Y、Sc 或混掺)[10]、铝酸盐($CaReAlO_4$，其中 Re 为 Y、Gd 或混掺)[11-13]、无序 CNGG 型石榴石[14-15]以及钨酸盐材料[16]。一方面通过 Tm/Ho 共掺或者基质材料自身强的晶格场作用实现激光发射波长大于 2 μm，来避开大气中水的吸收峰，另一方面，基质材料对于激活离子的光谱展宽效应，也是获得该波段超短飞秒脉冲产生的关键因素。这为后续新材料的开发提供重要方向引导。

具有钙钛矿结构的新型 $GdScO_3$基质材料(Pnma 空间群)，具有稳定的物化性能和低声子能量($481\ cm^{-1}$)[17]，且掺入的激活离子中心局部对称性中存在较大的低对称性畸变，从而导致发射光谱展宽[18]。近年来，稀土 Er^{3+}、Tm^{3+}、Yb^{3+}离子掺杂 $GdScO_3$晶体被逐一开发，其光学性能及连续激光性能也得到了初步研究[17-22]。其中，Tm:$GdScO_3$晶体的发射光谱范围可以覆盖 1550~2400 nm，实现了大于 300 nm 的激光波长调谐，说明该晶体是获得 2 μm 少周期脉冲产生的理想介质[21]。近期，本课题组研究了该晶体在$E//b$发光方向的锁模激光特性，得到了近 6 个光学周期的脉冲(44 fs)产生[23]，但是缺少该正交晶系其他偏振方向($E//a$和$E//c$)的锁模激光特性详细讨论。

本文详细研究了b切 Tm:$GdScO_3$晶体在$E//a$发光方向的被动锁模激光性能，采用了共振泵浦技术，较小的量子亏损有利于提高激光效率，并且相比于商业半导体激光器泵浦技术，可以有效降低晶体热效应对

收稿日期：2023-06-12；**修回日期**：2023-07-06；**录用日期**：2023-07-12；**网络首发日期**：2023-08-02

基金项目：国家自然科学基金(62075090，52032009)

通信作者：*yongguangzhao@yeah.net

激光性能的影响，有利于实现高功率激光输出，目前利用2 μm波段固体锁模激光器获得的高功率脉冲输出均是采用同带泵浦技术方案[24-26]。利用半导体可饱和吸收镜（SESAM）作为可饱和吸收体（SA），最终实现了锁模自动启并能长期稳定运转，在激光中心波长为2034 nm时实现了约9个光学周期的脉冲产生。然后，与其他发光方向的激光特性进行比较，使2 μm锁模激光性能研究更加系统，并进一步证实Tm∶$GdScO_3$晶体是一种优良的激光材料，具有获得少光学周期脉冲的能力。

2 实验装置

Tm∶$GdScO_3$固体锁模激光器实验装置如图1(a)所示，采用了像散补偿的标准X型谐振腔。为了降低量子亏损，提高激光斜效率，利用1700 nm的掺Er拉曼光纤激光器进行共振泵浦，与Tm∶$GdScO_3$晶体的第二吸收峰很好地重合，最高泵浦功率为5.2 W，光束质量因子为1.05。泵浦光经过焦距为75 mm的透镜聚焦在晶体上，光斑半径约为22 μm。激光增益介质采用掺杂原子数分数3%、沿b轴切割的Tm∶$GdScO_3$晶体，如图1(b)中插图所示，尺寸为3 mm×3 mm×6 mm，两端均未镀膜但以布儒斯特角切割，使出射激光偏振方向沿晶体a轴（$E//a$）。为了减小激光过程中晶体中的热负载，将激光晶体用铟铂包裹后放置在水冷夹具中，水冷工作温度设定为13 ℃。输入镜M1是曲率为−100 mm的凹面镜，在1900～2100 nm范围内镀有高反射膜，反射率大于99.9%。折叠镜M2和M3同样为凹面镜，曲率分别为−100 mm和−150 mm，所有腔镜均镀有1850～2200 nm的高反介质膜。输出镜（OC）为平镜，透过率分别为0.5%和1%。采用SESAM作为可饱和吸收体来启动和稳定锁模，该SESAM包含两个8.5 nm厚的InGaAsSb量子阱和一个50 nm的覆盖层，在2080 nm处具有97%的线性反射率[27]。激光通过腔镜M3在SESAM上再次形成第二束腰，光斑半径约为70 μm。为了补偿腔内色散，在谐振腔另一臂引入啁啾镜（CM1和CM2），每次经啁啾镜反射可提供的群延迟色散（GDD）均为−125 fs^2，优化后反射次数为4，即腔内往返总的GDD为−1000 fs^2。总物理腔长约为2 m，根据ABCD传输矩阵理论可以计算出腔内不同位置的光斑尺寸，得到在晶体上x和y方向上的激光斑半径分别为29 μm和56 μm。

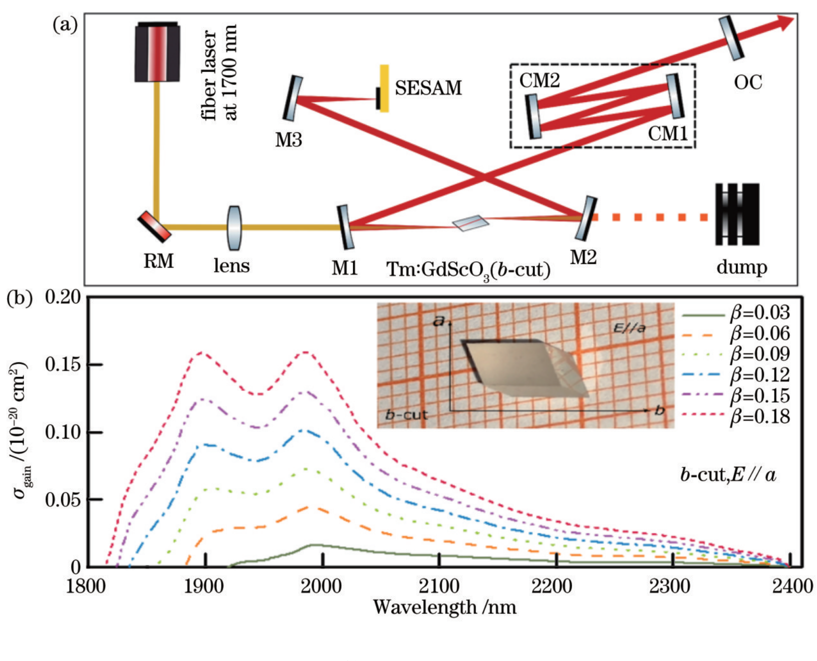

图1 实验装置和结果。(a)Tm∶$GdScO_3$固体锁模激光器装置图；(b)不同β值下的增益截面光谱图

Fig. 1 Experimental setup and results. (a) Schematic of Tm∶$GdScO_3$ solid-state mode-locked laser; (b) gain cross section spectra with different β values

激光晶体的吸收和受激发射截面大小是衡量其产生激光优劣性能的重要参数，根据测量的吸收和发射截面[21]，采用公式$\sigma_{gain}=\beta\sigma_{se}-\left(1-\beta\right)\sigma_{abs}$，计算了在不同上能级反转粒子数比率($\beta$)下的增益光谱，式中，$\sigma_{gain}$为增益截面，$\sigma_{abs}$和$\sigma_{se}$为吸收截面和发射截面，$\beta$为反转粒子数比率。如图1(b)所示，Tm∶$GdScO_3$在$E//a$偏振方向的增益谱线平坦且较宽，当$\beta=0.03$时，增益光谱波长覆盖范围从1922 nm扩展至2400 nm，增益光谱范围超过了450 nm，理论上可以支持2 μm波段小于5个光学周期的飞秒脉冲产生。

3 结果与分析

实验中，首先采用1%透过率的输出镜，对连续激光进行功率优化以使激光运转在低损耗区，最大连续

输出功率为 0.74 W，相应的谐振器损耗为 1.31%。随后，在腔内放入 SESAM 和啁啾镜对来研究 $Tm:GdScO_3$ 锁模激光性能，通过调节腔镜 M1 和 M2 之间的距离实现了稳定的锁模激光运转。在最高吸收泵浦功率为 3.14 W 时，输出激光的平均功率为 89 mW，相应的脉冲能量为 1.24 nJ，峰值功率为 17.4 kW。从图 2(a)可以看出，锁模光谱的中心波长位于 2052 nm，FHWM 为 78 nm，通过双曲正割函数($sech^2$)对测量光谱进行拟合，光谱形状与 $sech^2$ 型轮廓吻合良好。进一步利用自相关仪测量了时域信息，干涉自相关轨迹如图 2(b)所示，$sech^2$ 函数拟合后脉冲宽度为 63 fs，时间带宽积(TBP)为 0.35，非常接近傅里叶变换的极限 0.315，说明了锁模脉冲中几乎不包含啁啾成分。图 2(b)中的插图为长时间尺度(± 7.5 ps)下自相关轨迹，可以看出是一个干净、稳定的单脉冲，没有包含任何子脉冲。计算了在晶体上的激光强度，约为 66 GW/cm^2，高激光强度有利于增强克尔透镜(Kerr-lens)效应和自相位调制(SPM)效应。但当去掉 SESAM 可饱和吸收体之后，没有实现纯的 Kerr-lens 锁模，如果继续提升激光功率则受限于泵浦功率水平。

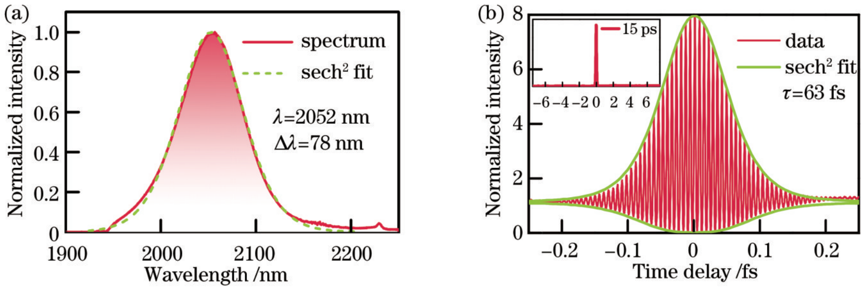

图 2　透过率 1% 时 SESAM $Tm:GdScO_3$ 锁模激光器。(a)光谱；(b)自相关轨迹[插图：对应的长时间尺度(±7.5 ps)下的自相关轨迹]

Fig. 2　SESAM mode-locked $Tm : GdScO_3$ crystal laser with transmittance of 1%. (a) Optical spectrum; (b) autocorrelation trace [inset: corresponding long-scale (± 7.5 ps) autocorrelation trace]

为了增强自相位调制效应来进一步缩短激光脉冲，选取更低透过率(0.5%)的输出镜提高腔内功率密度。在吸收泵浦功率为 3.26 W 时，平均输出功率降低至 38 mW，单脉冲能量为 0.53 nJ，峰值功率为 7.8 kW。此时，锁模光谱如图 3(a)所示，中心波长位于 2034 nm，通过双曲正割曲线拟合可以看出，光谱具有较好的 $sech^2$ 型轮廓，FWHM 为 80 nm。采用自相关测量来对锁模脉冲的时域信息进行表征，如图 2(b)所示，以 $sech^2$ 函数进行拟合，得到脉冲宽度为 60 fs，相应的 TBP 为 0.35，同样接近傅里叶转换极限。同时，测量了长时间尺度上的强度自相关曲线，如图 3(b)中的插图所示，在 15 ps 范围内没有任何子脉冲出现，是一个干净的单脉冲。遗憾的是通过降低透过率脉冲宽度没有实现明显的压缩，此时计算了晶体上的激光强度约为 59 GW/cm^2，相比于透过率为 1% 的情况，较小的激光强度未能有效激发介质强的非线性效应，这可能是导致减小透过率后脉宽没有出现明显缩短的原因。

在同样透过率(0.5%)下，本文对比了 $E//a$ 与 $E//b$ 发光方向的锁模激光特性，发现其锁模激光性能相似，均具有获得少周期脉冲的能力，但两种方向下获得的最短脉冲宽度仍有差别，主要归因于以下三方面：1)不同切向下材料的光谱特性不同，在同样的反转粒子数比率(β=0.03)下，$E//b$ 发光方向具有更宽的增益光谱，总增益光谱范围超过 550 nm[21]，而 $E//a$ 方向总增益光谱范围约为 500 nm，并且 $E//b$ 方向的增益截面比 $E//a$ 方向大，大且平滑的增益截面有利于实现超短脉冲输出。2)两种切向下腔内的功率密度不同，由于晶体在该波段的非线性折射率未知，无法直接对比两种切向下腔内的非线性效应，但可以计算出 $E//b$ 方向与 $E//a$ 方向在晶体上的激光强度分别为 123 GW/cm^2 和 59 GW/cm^2，更大的激光强度更有利于增强 SPM 效应，实现光谱展宽。最后，由于该晶体在 2 μm 波段的色散参数尚不明确，实验中通过啁啾镜对腔内色散进行补偿管理，对于 $E//b$ 方向利用啁啾镜只提供了 −500 fs^2 的负色散就获得了稳定的锁模脉冲，在 $E//a$ 方向下，本文尝试引入 −500 fs^2 的色散量，但锁模脉冲不稳定，因此，在该方向下通过优化腔内色散共引入 −1000 fs^2 的负色散，较大的色散补偿虽然有利于获得稳定的锁模脉冲，但会影响时域脉冲展宽。综上可知，通过对该晶体不同偏振方向下的锁模激光性能进行分析，证实了 $E//a$ 发光方向下 $Tm:GdScO_3$ 晶体也具有获得少光学周期脉冲的能力。

为了验证 $Tm:GdScO_3$ 晶体锁模激光器的稳定性，分别用射频仪、数字示波器以及光电探头记录了不同时间尺度下的频谱和脉冲序列。图 4(a)和图 4(b)展示了在 10 ns/div 和 10 ms/div 扫描范围下的锁模脉冲序列，锁模脉冲稳定性较好，没有发现任何调 Q 脉冲包络。如图 4(c)所示，测量了锁模稳定运转下的射频谱，分辨率带宽(RBW)设置为 300 Hz，激光重复频率测定为 71.6 MHz，信噪比大于 65 dBc。图 4(d)记录了 1 GHz 跨度范围内的射频谱，RBW 为 300 kHz，高对比度和接近恒定的谐波信号说明了锁模的稳定性很

高，可持续数小时，并且能够自启动。

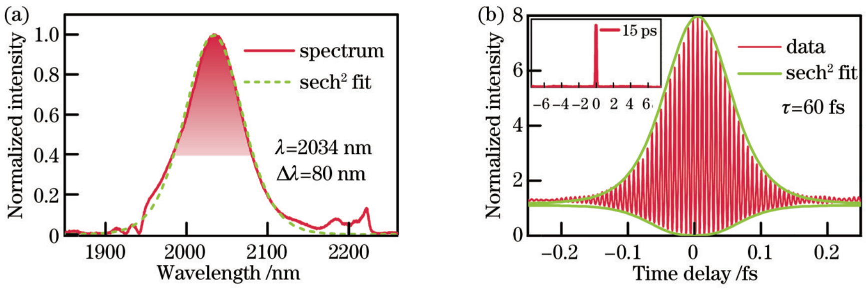

图3 透过率0.5%时SESAM Tm:$GdScO_3$锁模激光器。(a)光谱；(b)自相关轨迹[插图：对应的长时间尺度(±7.5 ps)自相关轨迹]

Fig. 3 SESAM mode-locked Tm：$GdScO_3$ crystal laser with transmittance of 0.5%. (a) Optical spectrum; (b) autocorrelation trace [inset: corresponding long-scale (± 7.5 ps) autocorrelation trace]

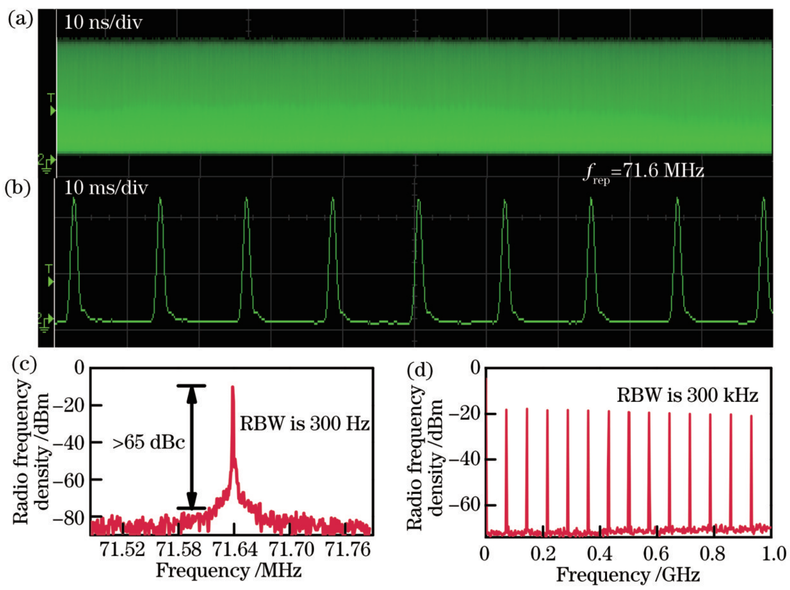

图4 SESAM锁模Tm:$GdScO_3$激光器。(a)纳秒和(b)毫秒时间尺度上的脉冲序列；(c)300 kHz和(d)1 GHz范围内的射频光谱

Fig. 4 SESAM mode-locked Tm：$GdScO_3$ laser. Pulse train on (a) nanosecond and (b) millisecond time scale; radio frequency spectra in the range of (c) 300 kHz and (d) 1 GHz

4 结　　论

本文采用具有钙钛矿结构的新型Tm:$GdScO_3$晶体作为增益介质，对$E//a$发光方向的锁模激光性能进行了详细研究，实现了脉冲宽度低于百飞秒的超快激光输出。通过平衡晶体的非线性效应和腔内的群延迟色散，在小透过率输出镜(0.5%)下，获得了60 fs的脉冲激光，约9个光学周期，光谱半峰全宽为80 nm。对比了该晶体其他偏振方向的锁模激光性能，目前，$E//b$发光方向已经获得了约6个光学周期的脉冲激光，遗憾的是，$E//c$发光方向未能实现锁模脉冲输出。此外，为了获得更短的锁模脉冲，未来可采用高功率泵浦源来激发更强的非线性效应，增强腔内SPM效应实现光谱展宽。通过对该晶体各发光方向下飞秒脉冲特性的补充与完善，证实了Tm:$GdScO_3$晶体在$E//a$偏振方向下的锁模激光性能与$E//b$偏振方向相似，也具有获得飞秒量级脉冲的潜力，是一种非常有发展前景的激光材料。

参 考 文 献

[1] Smolski V O, Yang H, Gorelov S D, et al. Coherence properties of a 2.6-7.5 μm frequency comb produced as a subharmonic of a Tm-fiber laser[J]. Optics Letters, 2016, 41(7): 1388-1391.

[2] Gattass R R, Mazur E. Femtosecond laser micromachining in transparent materials[J]. Nature Photonics, 2008, 2(4): 219-225.

[3] Chan V W S. Optical space communications[J]. IEEE Journal of Selected Topics in Quantum Electronics, 2000, 6(6): 959-975.

[4] Petrov V. Frequency down-conversion of solid-state laser sources to the mid-infrared spectral range using non-oxide nonlinear crystals[J]. Progress in Quantum Electronics, 2015, 42: 1-106.

[5] 蔡宇航，张俊旋，陈晓，等. 侧面抽运(Tm，Ho)：YLF晶体传导冷却百纳秒脉冲激光器[J]. 中国激光，2021，48(13): 1301005.
Cai Y H, Zhang J X, Chen X, et al. Side-pumped, conductively cooled (Tm, Ho): YLF pulsed laser with more than one-hundred-nanosecond pulse width[J]. Chinese Journal of Lasers, 2021, 48(13): 1301005.

[6] 吴鸿春. Tm:YLF 激光腔内泵浦 2.1 μm Ho:YVO4 激光器[J]. 中国激光, 2022, 49(23): 2301009.
Wu H C. Tm:YLF laser intracavity pumped 2.1 μm Ho:YVO_4 laser[J]. Chinese Journal of Lasers, 2022, 49(23): 2301009.

[7] 樊雨晴, 施翔春, 刘晶, 等. 2 μm 波段单掺铥脉冲固体激光器研究进展[J]. 激光与光电子学进展, 2023, 60(7): 0700003.
Fan Y Q, Shi X C, Liu J, et al. Research progress of Tm-doped pulsed solid-state lasers in 2 μm band[J]. Laser & Optoelectronics Progress, 2023, 60(7): 0700003.

[8] Pinto J F, Rosenblatt G H, Esterowitz L. Continuous-wave mode-locked 2-μm Tm:YAG laser[J]. Optics Letters, 1992, 17(10): 731-732.

[9] Wang Y C, Chen W D, Mero M, et al. Sub-100 fs Tm:$MgWO_4$ laser at 2017 nm mode locked by a graphene saturable absorber[J]. Optics Letters, 2017, 42(16): 3076-3079.

[10] Kränkel C. Rare-earth-doped sesquioxides for diode-pumped high-power lasers in the 1-, 2-, and 3-μm spectral range[J]. IEEE Journal of Selected Topics in Quantum Electronics, 2015, 21(1): 250-262.

[11] Zhao Y G, Wang Y C, Zhang X Z, et al. 87 fs mode-locked Tm, Ho:$CaYAlO_4$ laser at ~2043 nm[J]. Optics Letters, 2018, 43(4): 915-918.

[12] Wang Y C, Loiko P, Zhao Y G, et al. Polarized spectroscopy and SESAM mode-locking of Tm, Ho: CALGO[J]. Optics Express, 2022, 30(5): 7883-7893.

[13] Wang L, Chen W D, Zhao Y G, et al. Sub-50 fs pulse generation from a SESAM mode-locked Tm, Ho-codoped calcium aluminate laser[J]. Optics Letters, 2021, 46(11): 2642-2645.

[14] Wang Y C, Zhao Y G, Pan Z B, et al. 78 fs SWCNT-SA mode-locked Tm: CLNGG disordered garnet crystal laser at 2017 nm[J]. Optics Letters, 2018, 43(17): 4268-4271.

[15] Zhao Y G, Wang Y C, Chen W D, et al. 67-fs pulse generation from a mode-locked Tm, Ho: CLNGG laser at 2083 nm[J]. Optics Express, 2019, 27(3): 1922-1928.

[16] Petrov V, Wang Y C, Chen W D, et al. Sub-100-fs bulk solid-state lasers near 2-micron[J]. Proceedings of SPIE, 2019, 11209: 112094G.

[17] Li S M, Fang Q N, Zhang Y H, et al. 2 μm Ultrabroad spectra and laser operation of Tm: $GdScO_3$ crystal[J]. Optics & Laser Technology, 2021, 143: 107345.

[18] Zhang Y H, Li S M, Du X, et al. Yb: $GdScO_3$ crystal for efficient ultrashort pulse lasers[J]. Optics Letters, 2021, 46(15): 3641-3644.

[19] Li S M, Tao S L, Zhang S Y, et al. Tm:$GdScO_3$: a promising crystal for continuous-wave and passively *Q*-switched laser at 2 μm[J]. Optics & Laser Technology, 2022, 156: 108628.

[20] Liu J, Li S M, Qian C P, et al. High-beam-quality 2 μm tunable Tm: $GdScO_3$ laser pumped by a 793 nm laser diode[J]. Laser Physics Letters, 2022, 19(11): 115801.

[21] Song Q S, University T, Zhang N, et al. Efficient continuous wave and broad tunable lasers with the Tm:$GdScO_3$ crystal[J]. Optics Letters, 2023, 48(3): 640-643.

[22] Hou W T, Zhao H Y, Qin Z P, et al. Spectroscopic and continuous-wave laser properties of Er:$GdScO_3$ crystal at 2.7 μm[J]. Optical Materials Express, 2020, 10(11): 2730-2737.

[23] Zhang N, Song Q S, et al. 44-fs pulse generation at 2.05 μm from a SESAM mode-locked Tm: $GdScO_3$ laser[J]. Optics Letters, 2023, 48(2): 510-513.

[24] Zhang N, Wang Z X, Liu S D, et al. Watt-level femtosecond Tm-doped "mixed" sesquioxide ceramic laser in-band pumped by a Raman fiber laser at 1627 nm[J]. Optics Express, 2022, 30(13): 23978-23985.

[25] Yao W C, Wang Y C, Tomilov S, et al. 8.7-W average power, in-band pumped femtosecond Ho: CALGO laser at 2.1 μm[J]. Optics Express, 2022, 30(23): 41075-41083.

[26] Tokurakawa M, Fujita E, Kränkel C. Kerr-lens mode-locked Tm^{3+}: Sc_2O_3 single-crystal laser in-band pumped by an Er: Yb fiber MOPA at 1611 nm[J]. Optics Letters, 2017, 42(16): 3185-3188.

[27] Paajaste J, Suomalainen S, Härkönen A, et al. Absorption recovery dynamics in 2 μm GaSb-based SESAMs[J]. Journal of Physics D: Applied Physics, 2014, 47(6): 065102.

2 μm Mode-Locked Tm : $GdScO_3$ Laser

Wei Wenlong[1], Zhang Ning[1], Song Qingsong[2], Liu Jian[1], Wang Zhanxin[1], Zhao Yongguang[1*], Xu Xiaodong[1], Xue Yanyan[2], Xu Jun[2]

[1] *Jiangsu Key Laboratory of Advanced Laser Materials and Devices, Jiangsu Normal University, Xuzhou* 221116, *Jiangsu, China*;

[2] *School of Physics Science and Engineering, Institute for Advanced Study, Tongji University, Shanghai* 200092, *China*

Abstract

Objective Femtosecond lasers in the 2 μm spectral range have important applications in various fields, such as molecular ultrafast dynamics research, high-precision organic material processing, and free-space optical communication. They can also be utilized as a pump source for optical parametric oscillators to achieve mid-IR laser generation through frequency down-conversion, which is a current frontier hotspot in laser technology. Since the commercialization of semiconductor preparation processes and the rapid development of new low-dimensional materials, passively mode-locked solid-state lasers gradually became one of the main means to obtain femtosecond pulses at 2 μm from 1980. Currently, the main host materials that can produce sub-100 fs pulse output based on Tm^{3+}- or Tm^{3+}, Ho^{3+} co-doped laser materials are sesquioxides (Re_2O_3, where Re is Lu, Y, Sc, or their mixture), aluminates ($CaReAlO_4$, where Re is Y, Gd, or mixture), disordered CNGG-type garnets, and tungstate materials. The laser emission wavelength should be above 2 μm to avoid the structured water vapor air absorption and obtain ultrashort femtosecond pulses in the 2 μm spectral range, which can be realized by Tm/Ho co-doping or the strong lattice field effect of the host materials. Meanwhile, the spectral broadening effect of the host material on the active ions is also a key factor to achieve femtosecond pulses in this region. Therefore, it is necessary to explore new materials with flat and broadband gain spectra. In this study, we investigate the passively mode-locked performance of the new Tm∶$GdScO_3$ crystal with orthorhombic perovskite structure and a flat broadband (>450 nm) gain spectrum to demonstrate that it is an ideal laser material for achieving few-optical-cycle pulses in the 2 μm spectral range.

Methods A standard astigmatically compensated X-shaped cavity is employed for the experiments (Fig. 1). To reduce the quantum loss and improve the laser slope efficiency, we adopt an Er-doped Raman fiber laser at 1700 nm for in-pumping and match well with the second absorption peak of the Tm∶$GdScO_3$ crystal. The maximum pump power is 5. 2 W and the beam quality factor M^2 is 1. 05. The pump light is focused on the crystal through a lens with a focal length of 75 mm and a beam radius of 22 μm. The gain medium is a Tm-doped $GdScO_3$ crystal with atomic fraction of 3% and dimensions of 3 mm×3 mm×6 mm. It is cut along the b-axis at Brewster's angle to enforce the laser polarization along the b-axis ($E//a$). To mitigate the thermal load in the crystal during the laser operation, we wrap the laser crystal with indium platinum and place it in a water-cooled fixture with a working temperature of 13 ℃. A semiconductor saturable absorber mirror (SESAM) is utilized as a saturable absorber (SA) to initiate and stabilize the mode-locking (ML). Chirped mirrors (CM1 and CM2) are introduced in the other arm of the cavity to compensate for the intracavity dispersion. The total physical cavity length is about 1. 9 m. The laser beam radii in the sagittal and tangential planes on the crystal are 29 μm and 56 μm, respectively.

Results and Discussions Initially, a 1% output coupler (OC) is employed for laser operation. At the maximum absorbed pump power, the laser delivers 0. 74 W power in the continuous wave (CW) regime. With an optimized configuration for dispersion compensation of two beam bounces on CM1 and CM2, the physical cavity length amounts to 1. 9 m, leading to a pulse repetition rate of 71. 6 MHz. The mode-locked laser is self-starting and stable for hours. At an absorbed pump power of 3. 14 W, it delivers an average output power of 89 mW, corresponding to a pulse energy of 1. 24 nJ. The measured optical spectrum has a peak wavelength of 2052 nm and a full width at half maximum (FWHM) of 78 nm. The corresponding interferometric autocorrelation trace is shown in Fig. 2(b). The nearly perfect fits of the envelopes assuming a $sech^2$-pulse profile and the expected 8∶1 peak-to-background ratio indicate chirp-free pulses. The deconvolved pulse duration (FWHM intensity) amounts to 63 fs. Single-pulse ML without any temporal satellites is confirmed by the measured intensity autocorrelation trace on a 15 ps-long time scale (Fig. 2).

With the same configuration, ML of the same Tm∶$GdScO_3$ crystal is thereafter investigated by the 0. 5% OC. We obtain an average output power of 38 mW at an absorbed pump power of 3. 26 W, with a single pulse energy of 0. 53 nJ and a peak power of 7. 7 kW. At this time, the central wavelength is located at 2034 nm with an FWHM of 80 nm. The hyperbolic secant curve fit shows a good $sech^2$-type profile. Self-correlation measurements are performed to characterize the time-domain information of the mode-locked pulse, which is fitted with a $sech^2$ function. Meanwhile, a pulse width of 60 fs is obtained, with a corresponding TBP of 0. 35, again close to the Fourier transition limit. Compared to the case of a 1% transmittance, the smaller laser intensity fails to excite the strong nonlinear effects of the medium, which may be the reason why the pulse width does not significantly shorten after reducing the transmittance (Fig. 3).

To characterize the stability of the mode-locked Tm∶$GdScO_3$ laser, we record radio frequency (RF) spectra of the shortest pulses on different span ranges. The fundamental beat note at 71. 6 MHz exhibits an extinction ratio of more than 65 dBc above the noise level. The high contrast and near constant harmonic beat notes on a 1 GHz span range are evidence of stable ML operation. Furthermore, no Q switching behavior and multi-pulse instabilities are observed in the recorded uniform real-time pulse trains on different time scales (Fig. 4).

Conclusions In summary, we report on a SESAM mode-locked Tm∶$GdScO_3$ crystal laser in-band pumped by a Raman fiber laser at 1700 nm. The flat broadband gain spectrum of the Tm∶$GdScO_3$ crystal is well utilized in the mode-locked laser operation, and an average output power of 38 mW is achieved for transform-limited 60 fs pulses at a repetition rate of 71. 6 MHz, corresponding to a spectral bandwidth of 80 nm. Our results demonstrate that Tm∶$GdScO_3$ crystal is a promising candidate for generating few-optical-cycle pulses in the 2 μm spectral range. Thus, it has potential applications in scientific research such as molecular ultrafast dynamics and high-resolution molecular spectroscopy.

Key words solid-state mode-locked laser; Tm∶$GdScO_3$ crystal; ultrashort pulse